AAS 23-301 (Preprint)

PASSIVE STABILIZATION OF ROTATING SPACECRAFT USING DYNAMIC FLUID-PRESSURE EQUILIBRIUM

Matthew M. Wittal,* Taylor A. Peterson,† Sara M. Tavarez-Garcia,‡ Michael P. Kinzel§

Rotating spacecraft can provide artificial gravity for long-term space missions, but the design of a Guidance and Control scheme for these vehicles is nuanced. For a three-segment vehicle with the propulsion element located at the center of mass, the vehicle must stabilize itself about this point even in the event of various off-nominal circumstances. Thus, a robust and passive spin stabilization system is needed. In this paper, the dynamics of this system are explored and constraints are placed on the performance and controllability. A controller is thus developed based on assumptions regarding the fluid transfer between elements, and the result is simulated. Generalized methodology is then extracted and extended applications are explored, such as a conceptual fluid ring and active mass displacement for attitude control.
Keywords:Dynamics, tether, spin stabilization

INTRODUCTION

Travel between the Earth and Mars takes many months [1] and to ensure safety, it is critical for these systems to improve for the reliability of space systems during long-term, deep space missions. Some work has been done on wobble stabilization [2, 3], but while these works are similar to the topic of this paper, they do not completely cover the methods explored here. For this paper, a specific inquiry is posed: can the distribution of fluids between elements of a tethered system be used to passively stabilize a rotating spacecraft?

Tethered spacecrafts are systems of two or more bodies connected through long, high-strength cables in a space environment. The dynamics and applications of these systems are considered in this study to explore new methods for passive spin stabilization. Since efforts for future deep space missions are currently under development, resource management for human life support and providing artificial gravity is a big concern. While other works have explored the use of active stabilization for tethered spacecraft [4], the objective of this study is to achieve the same effective stabilization and reliability without the need to use propellants or power.

To model the distribution of water and air between elements of a tethered system in a realistic way, analytical and computational fluid dynamics (CFD) models are developed. These models demonstrate the relocation of non-potable water alongside the spacecraft to balance the weight and therefore shift the center of mass as a method of passive stabilization using fluid transfer. The intention is to extend this method to include any mass transfer and any perturbation by first establishing a baseline dynamical model. Other work has looked at spacecraft configurations undergoing fluid transfer, specifically in the interest of understanding slosh dynamics [5, 6].

*Automation and Robotics Systems Engineer, Granular Mechanics and Regolith Operations Laboratory, NASA Kennedy Space Center, FL 32899, and Ph.D. Candidate, Embry-Riddle Aeronautical University, 1 Aerospace Blvd., Daytona Beach, FL 32114
†NASA Kennedy Space Center OSTEM Intern and Ph.D. Student, University of Central Florida, 4000 Central Florida Blvd, Orlando, FL 32816
‡OSTEM Intern, Granular Mechanics and Regolith Operations Laboratory, NASA Kennedy Space Center, FL, 32899 USA
§Associate Professor, University of Central Florida, 4000 Central Florida Blvd, Orlando, FL 32816

Significant efforts have been made to understand the behaviors of spinning, tethered systems since it is one of the primary keys to creating artificial gravity on long-distance travel through deep space. This method uses the fundamentals of centripetal force that simulates gravity inside the spacecraft [7–9].

One scientist that has explored this concept was American physicist Gerard K. O'Neill [10]. His concept, colloquially known as the "O'Neill cylinder", involved two parallel counter-rotating cylinders tethered to each other. This arrangement would keep the cylinders in place, counteract any wobble and create artificial gravity that would allow for a space settlement within the inner surface of each cylinder. This model would work by rotating about 28 times an hour to simulate the standard Earth gravity and would have an angular velocity of 2.8 degrees per second. It is believed that at these speeds, the central axis of the cylinders would be a zero-gravity region that could be used for experimental and operational research development.

Another useful concept that could be further developed on tethered systems is on-orbit manufacturing using variable gravity [11]. The concept of tethered systems has the potential to open up new possibilities in space exploration [12]. However, since efforts to understand the dynamics of a rotating, tethered spacecraft are still underway, the possibilities of manufacturing products on different gravity levels are still being explored, but they have a high potential to yield results that are unachievable on Earth. This provides a unique opportunity to create specialized hardware to fill current technological gaps and advance the efforts for sustainable resources to support human life during deep space travel.

Long-duration space travel includes a particular set of challenges and this paper seeks to propose a solution to several that apply to tethered systems. Space tethers [13] are versatile technology with valuable applications including, but not limited to, electrodynamic propulsion, momentum exchange between spacecraft, and formation flying. However, these methods do not completely consider the conditions posed in this study.

This paper explores passive stabilization strategies using a redesigned fluid management system. This method is ideal for being cost-effective and resourceful, while also allowing for reduced power consumption during long-term deep space missions.

DYNAMICS IN THE ROTATING FRAME

In a spinning system, the apparent acceleration experienced at any point along radius r, denoted as $[\ddot{r}]$, is expressed as

$$[\ddot{r}] = -\ddot{r} - \dot{\omega} \times r - 2\omega \times [\dot{r}] - \omega \times (\omega \times r) \tag{1}$$

such that the terms $-\ddot{r}$ is the acceleration of the rotating system, $-\dot{\omega} \times r$ is the Euler acceleration, $-2\omega \times [\dot{r}]$ is the coriolis acceleration, and $\omega \times (\omega \times r)$ is the centrifugal force. Considering this as a function only about one axis, the vector form stated above may be relaxed to express these dynamics in the form of

$$[\ddot{x}] = -\ddot{x} - \ddot{\theta}x - 2\dot{\theta}[\dot{x}] - \dot{\theta}^2 x \tag{2}$$

Such that x is the first axis of vector r in the rotating frame. For the system illustrated in Fig. 2, the systems acceleration, $\ddot{r} = \ddot{x} = 0$, and the angular acceleration $\dot{\omega} = \ddot{\theta} = 0$. This further simplifies the system to

$$[\ddot{x}] = -2\dot{\theta}[\dot{x}] - \dot{\theta}^2 x \tag{3}$$

A body frame $\mathcal{B}$ with an origin at the center of the propulsion element is defined, which is also the desired center of mass. The true center of mass with respect to this body frame is derived from the formula for the center of mass of a multi-body system expressed as

$$r_{cm} = \frac{1}{m_T} \sum_{i=1}^{n} m_i r_i \tag{4}$$

where n is the number of bodies. For this simplified example, we assume that the change in center of mass is small, and thus consider only the two bodies: the habitation element and the cargo element, neglecting the central propulsion element. The resulting expression is

$$r_{cm} = \frac{1}{m_T}(m_1 r_1 + m_2 r_2) \tag{5}$$

The rate of change of the center of mass as a function of time may then be expressed as

$$\dot{r}_{cm} = -\frac{r_T}{m_T}\dot{m}_1 \tag{6}$$

Taking again the derivative with respect to time and applying the chain rule,

$$\ddot{r}_{cm} = \frac{\mathrm{d}}{\mathrm{d}t}\dot{r}_{cm} = -\frac{r_T}{m_T}\ddot{m}_1 \tag{7}$$

This demonstrates that the change in the center of mass is linear if the mass flow rate is constant, or nonlinear directly as a function of the mass flow rate. However, since both mass m_T and the total distance r_T between the elements remain constant and in the body frame $r_2 = -(r_T - r_1)$, we can rewrite this expression as

$$r_{cm} = \frac{1}{m_T}\left(m_1 r_1 - (m_T - m_1)(r_T - r_1)\right) = r_T - r_1 - \frac{r_T}{m_T}m_1 \tag{8}$$

The time derivative of r_1 is expressed and the chain rule is applied as

$$\dot{r}_1 = \frac{\mathrm{d}r_1}{\mathrm{d}t} = \frac{\mathrm{d}r_1}{\mathrm{d}m_1}\frac{\mathrm{d}m_1}{\mathrm{d}t} = \frac{\mathrm{d}r_1}{\mathrm{d}m_1}\dot{m}_1 \tag{9}$$

where $\frac{\mathrm{d}m_1}{\mathrm{d}t} = \dot{m}_1$ and $\frac{\mathrm{d}r_1}{\mathrm{d}m_1} = -\frac{\mathrm{d}r_{cm}}{\mathrm{d}m_1}$. Eq. 6 may then be used to derive $\frac{\mathrm{d}r_1}{\mathrm{d}m_1} = \frac{r_T}{m_T}$. Eq. 9 is then inserted resulting in

$$\dot{r}_1 = \frac{r_T}{m_T}\dot{m}_1 \tag{10}$$

The expression for the $r_1(t)$ may be discretized as

$$r_1(t) = r_{1,0} + \dot{r_1}\mathrm{d}t = r_{1,0} + \dot{r}_{cm}\mathrm{d}t \tag{11}$$

However, if we assume our initial state is at the desired position of $r_1 = r_2$, then $r_1 = \frac{1}{2}r_T$ and this can be plugged in as well as the derived equation for $\dot{r_1}$ to yield

$$r_1(t) = \frac{r_T}{2} + \frac{r_T}{m_T}\dot{m}t \tag{12}$$

Which are the dynamics of the system in the uncontrolled system in the rotating frame with pressure or return mass dynamics considered.

FLUID DYNAMICS FOR SPIN STABILIZATION

To simplify the problem, it is assumed the liquid is an incompressible, laminar Newtonian fluid used to formulate the governing continuity and Navier-Stokes (NS) equations with a volume-of-fluid (VOF) framework to capture liquid and water. These equations essentially consider the system to have a conservation of global and liquid masses as well as the mixture momentum. The continuity, VOF equation, and NS equations are as follows, respectively,

$$\frac{\partial \rho}{\partial t} + \rho \boldsymbol{\nabla} v = 0 \tag{13}$$

$$\frac{\partial \rho\alpha}{\partial t} + \rho \boldsymbol{\nabla} \alpha v = 0 \tag{14}$$

$$\rho\left(\frac{\partial v}{\partial t} + v\boldsymbol{\nabla} v\right) = -\boldsymbol{\nabla} p + \mu \boldsymbol{\nabla}^2 v + \rho f_{body} \tag{15}$$

Simplifying even further, it is assumed the density of the liquid does not change. It is also known that f_{body} represents any external body forces, which in this case is gravity [14].

$$\frac{\partial u}{\partial x} + \frac{\partial v}{\partial y} + \frac{\partial w}{\partial z} = \nabla v = 0 \tag{16}$$

$$\rho(\frac{\partial v}{\partial t} + v\nabla v) = -\nabla p + \nabla^2 v - \rho g\hat{x} \tag{17}$$

Where $\hat{x}$ is the unit vector of the gravity direction. The laminar-flow assumption is guided by the expected Reynolds number (Re) values to observe in the system. Re is dependent on the fluid properties (i.e., ν), bulk flow velocity through the tether along with the tether's diameter and is given as

$$Re = \frac{V_{avg} D}{\nu}, \tag{18}$$

where V_{avg} is the average (or bulk) flow velocity, D is tether diameter, and ν is the kinematic viscosity of the fluid. Although not confirmed, the liquid flows is anticipated to flow at low speeds and the tether has a small diameter, Reynolds number falls under 2,300 which is expected to imply laminar flow. This assumption will be evaluated in the final product.

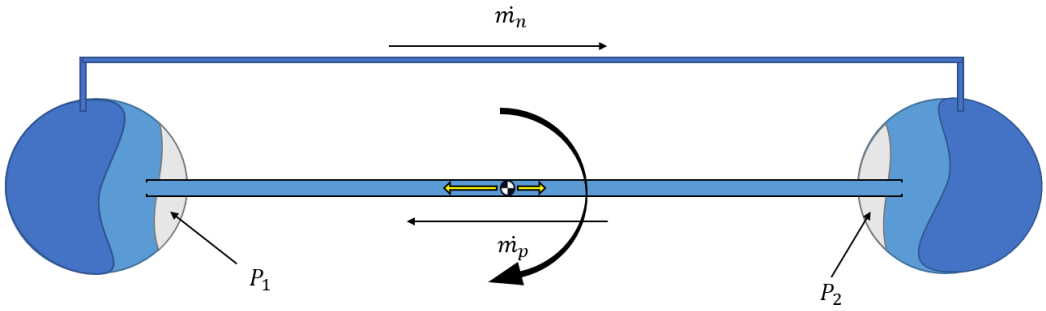

Figure 1: The internal diagram of the fluid flow between the elements in the rotating frame. Incompressible, potable water is flowed from the right to the left, increasing the mass of the left element and forcing the non-potable water back to the right as pressure increases.

The configuration of the fluid vessels is illustrated in Figure. 1. The non-potable fluid in the return is incompressible and isothermic, and thus the only considerations are the change in acceleration on the fluid container from the dynamical system and the change in pressure of the air in the tank. It is assumed that the mass of potable water flowing from right to left is driven by a pump and held constant and thus not affected by the change in pressure on either side. It is also assumed that both pipes are filled and have no air bubbles. At the start of the simulation, the right side contains 750kg of potable water and 450kg of non-potable water, while the left side contains 50kg of potable water and 250kg of non-potable water.

An augmented form of Bernoulli's principle is applied as

$$P_h + \frac{1}{2}\rho v^2 + \rho \ddot{r}_h r_h - \delta P dt = P_c + \frac{1}{2}\rho v^2 + \ddot{r}_c(R - r_h) \tag{19}$$

$$v = \text{sign}(P_h - P_c)\sqrt{||2\left(\frac{P_h - P_c}{\rho} + \ddot{r}_h r - \rho \ddot{r}_c(R - r_h)\right)||}$$

Using this, the return mass flow rate - that is, the mass flow rate of the non-potable water - may be modeled as a function of velocity, density, and cross-sectional area as

$$\dot{m}_n = v\rho A_r \tag{20}$$

The term δP in Eq. 19 is the augmentation to Bernoulli's equation that allows the consideration of energy loss due to viscous effects. For this, the Darcy-Weissbach equation is applied as

$$\delta P = \frac{f_D \rho v^2}{2 D_H} L \tag{21}$$

where L is the length of the tube, $f_D = \frac{64}{R_e}$ is the Darcy friction factor, and D_H is the hydraulic diameter. For small-diameter pipes such as what is considered in this work, the hydraulic diameter is taken to be equal to the pipe diameter D.

CASE STUDY

A concept model of a tethered spacecraft can be seen in Figure 2, where the shifted center of mass is exaggerated.

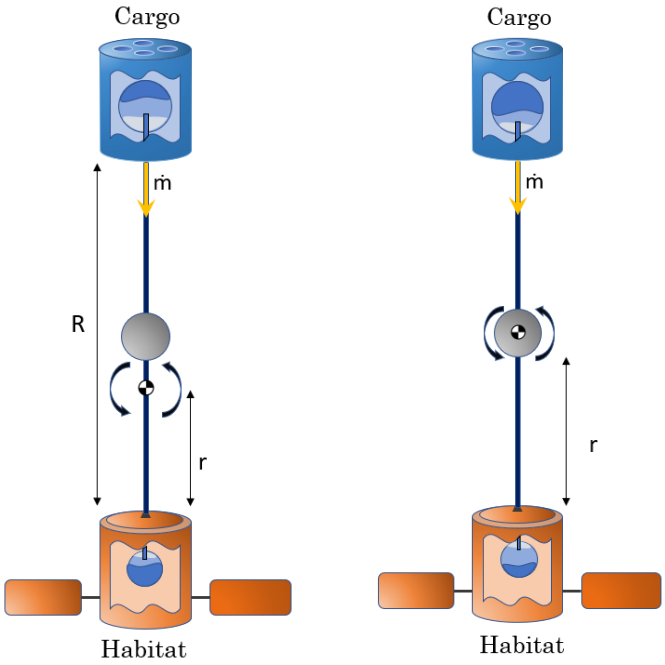

(a) Shifted Center of Mass (b) Corrected Center of Mass

Figure 2: Concept model of a tethered spacecraft

The conceptual extension of this system may be an annulus of fluid, a variation of which was explored for the purposes of attitude control by Nobari and Misra [15]. By exploring the passive asymptotic stability of a bi-nodal spinning system, it can be extended to multiple nodes, and then a continuum of time-varying mass. By exploring this parameter space, the implications to systems such as refuelers and manned spacecraft will be better understood.

Figure 3 shows the analysis of the motion of a tethered spacecraft when the center of mass is aligned with the geometric center of the system. This allows for the verification of our mathematical analysis shown before, simulating the rotation of the elements using their inertial frame and their rotating frame as references. The inertial frame illustrates the rotation of the system as a whole while it travels through space, while the rotating frame shows the wobble of the spinning axis as the center of mass slightly shifts.

Table 1: Spacecraft Properties

Habitat Element Values	
Dry Mass [kg]	$m_{s1} = 14500$
Fluid Mass [kg]	$m_{p1} = 500$
$\dot{m}$[kg/s]	$\dot{m} = 0.6$
Dimensions [m]	$r = 4$, $l = 8$
Tank Dimensions [m]	$r = 0.5$
Initial Inertia [kg m^2]	$J = \text{diag}([7604291,\ 7604291,\ 2975979])$
Cargo Element Values	
Empty Mass [kg]	$m_{s2} = 14000$
Fluid Mass [kg]	$m_{p2} = 1000$
$\dot{m}$[kg/s]	$\dot{m} = -0.6$
Dimensions [m]	$r = 4$, $l = 8$
Tank Dimensions [m]	$r = 0.65$
Initial Inertia [kg m^2]	$J = \text{diag}([884642,\ 576846,\ 655827])$
Propulsion Element Values	
Empty Mass [kg]	$m_{s2} = 5000$
Propellant Mass [kg]	$m_{p2} = 5000$
$\dot{m}$[kg/s]	$\dot{m} = 0$
Dimensions [m]	$r = 4$, $l = 2$
Initial Inertia [kg m^2]	$J = \text{diag}([884642,\ 576846,\ 655827])$

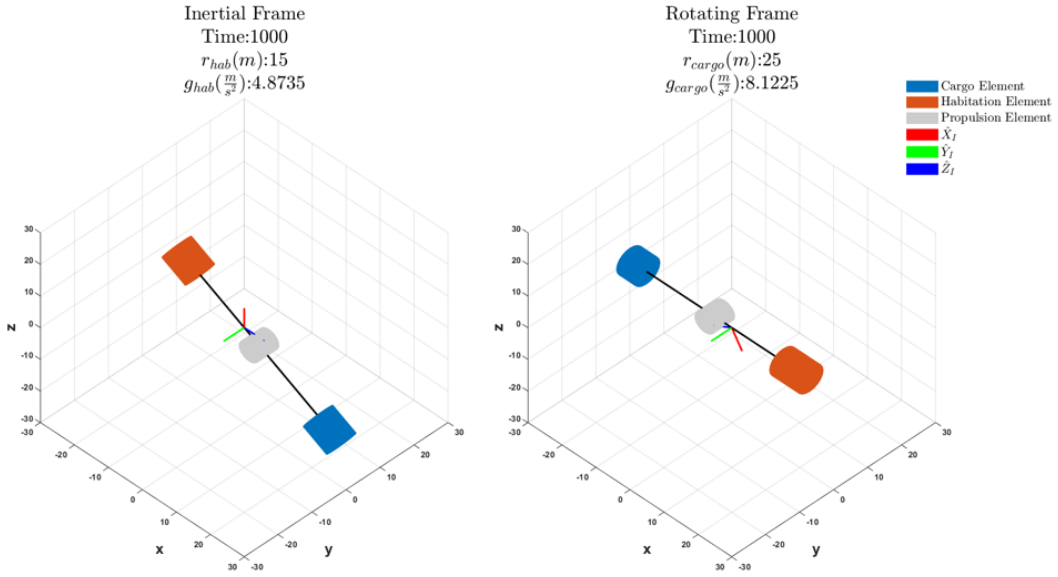

Figure 3: The result of about 16 minutes of simulation. As mass flows from the cargo element to the habitation element, the displacement of mass results in a significant change in perceived gravity.

COMPUTATIONAL FLUID DYNAMICS SIMULATION

In order to quantify the fluid dynamics of the rotating system, a CFD simulation is being developed. The system was simplified to only the cargo and habitat element connected via tether with a pressure release line connection, shown above in Figure 1. After initial simulations with a coarser mesh, the mesh was refined to a base size of 0.01 m and a maximum cell size of 0.01 m. A close up of the mesh grid, including boundary prism

layers, can be seen in Figure 4. The simulation uses an adaptive mesh, meaning the mesh is automatically refined in needed areas as the simulation runs. The section about $\frac{3}{4}$ of the way up the tank shows the adaptive mesh creating a finer mesh where the two phases (water and air) meet to increase accuracy in the region.

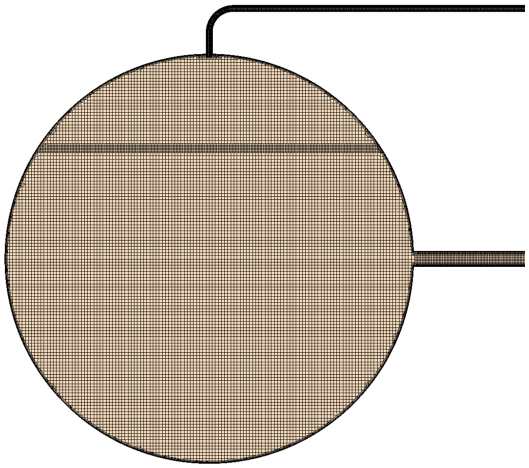

Figure 4: Close up of the mesh on the cargo element, showing the adaptive mesh.

The simulation uses a laminar flow with volume of fluid (VOF) and multiphase flow methods, which utilize the continuity and NS equations shown in the Fluid Dynamics For Spin Stabilization section above. For an initial simulation, the fill level was held at about 80% liquid and initialized in a completely settled state, shown in Figure 5. The rotation is set at the geometric center for this simulation to understand the fluid dynamics of the system.

Figure 5: Initial CFD state of about 80% liquid fill.

The dimensions of the model are the same as in Table 1. Since the system had an initial liquid fill, the boundary condition for each part is set as a wall to ensure no loss of liquid. It is modeled with a multiphase interaction of water and air with a velocity from left to right through the tether and the rotation rate set to 0.57 $\frac{\text{deg}}{\text{s}}$. The simulation uses a segregated flow solver and a first-order temporal discretization implicit unsteady solver.

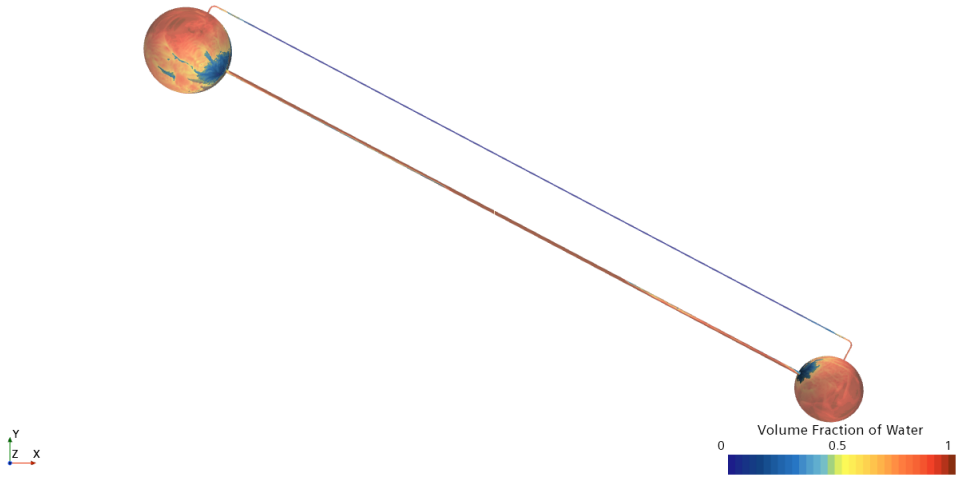

Figure 6: Volume fraction of water in CFD simulation after rotation.

Figure 6 shows the volume fraction of water after a short time. It is shown that the liquid is now unsettled and in the process of transferring from the cargo element to the habitat element. During this, the pressure force was observed in the cargo element, shown in Figure 7.

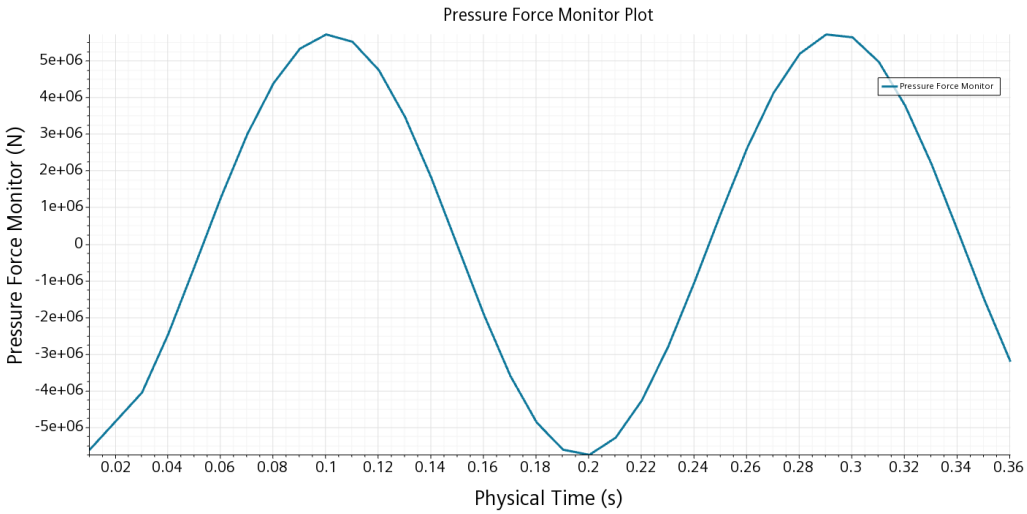

Figure 7: Pressure force tracked inside of the cargo element against time.

The pressure force is tracked in newtons (N) and shows an oscillatory motion as the system rotates. The force is slightly high as 1 $\frac{\text{N}}{\text{m}^2}$ is equal to 1 Pa. This could be due to a mixture of an issue with the set-up or the small tether diameter, which is set at 5 cm for this simulation. Due to the fine mesh, the computation time is greatly increased. The physical time of the system is currently short, but simulations are still in process.

NUMERICAL SIMULATION RESULTS AND DISCUSSION

Simulation of the dynamical system using the analytical formulation described in Section focused on total system mass, with a specific interest in the relative diameters of the pump and return lines $\frac{D}{D_o}$, where D is the diameter of the non-potable return water line and D_o is the fixed diameter of the pump line, set to 10 cm.

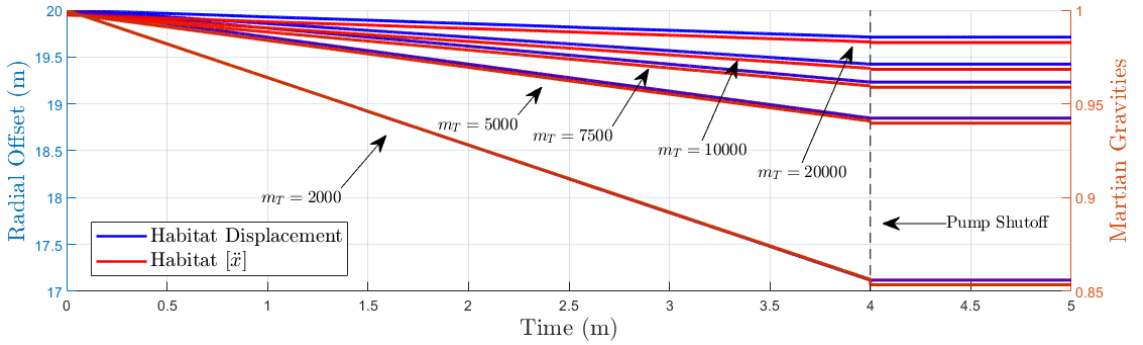

Figure 8: How total system mass affects radial displacement given the same mass flow rate. $m_T = 2000$ kg is almost exclusively the mass of the liquid while $m_T = 20000$ kg is the complete Mars transfer vehicle with full propellant.

For the case where there is no return line, variation in total system mass had a nonlinear relationship with the offset of the system during a 4-minute pump at $0.6\frac{\text{kg}}{\text{s}}$. As illustrated in Figure 8, a radial offset of nearly 3 m was achieved when considering a system mass of $2,000$ kg, which is little more than just the mass of the two tanks. A more realistic system mass of $20,000$ kg yields a significantly smaller radial offset with steps in between being spread out in a logarithmic pattern approaching 0.

Setting the mass equal to $20,000$ kg, the results of exploring the relationship between the stability of the system and the return pipe diameter is illustrated in Figure 9 and 10. In general, the larger the return line, the more quickly the system restabilizes about the desired geometric center. However, with return lines greater than $\frac{D}{D_o} = 1$, slosh occurs between the tanks. It is worth noting that this simulated slosh between tanks does not dampen in these simulations due to the step size, and smaller step sizes generate smaller slosh amplitudes, thus it is expected that in a real scenario, these dynamics would dampen rather quickly (< 60 s). Future work

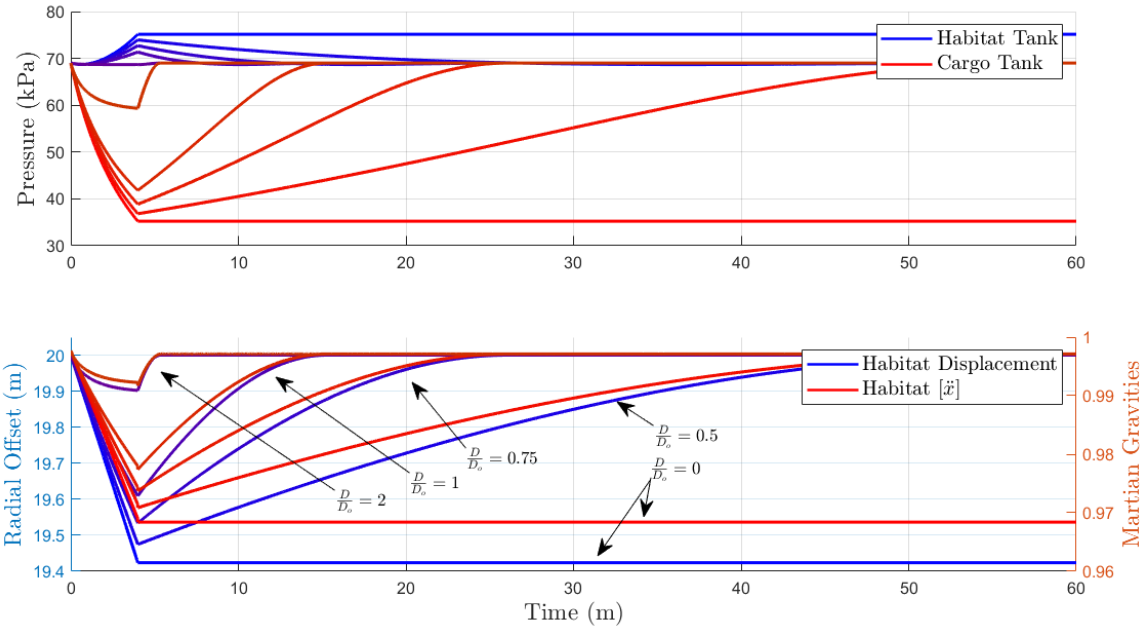

Figure 9: (Top) The pressure in each of the tanks over time of the uncontrolled system.
(Bottom) The radial offset of the system and the acceleration felt at either extreme of the spinning system.

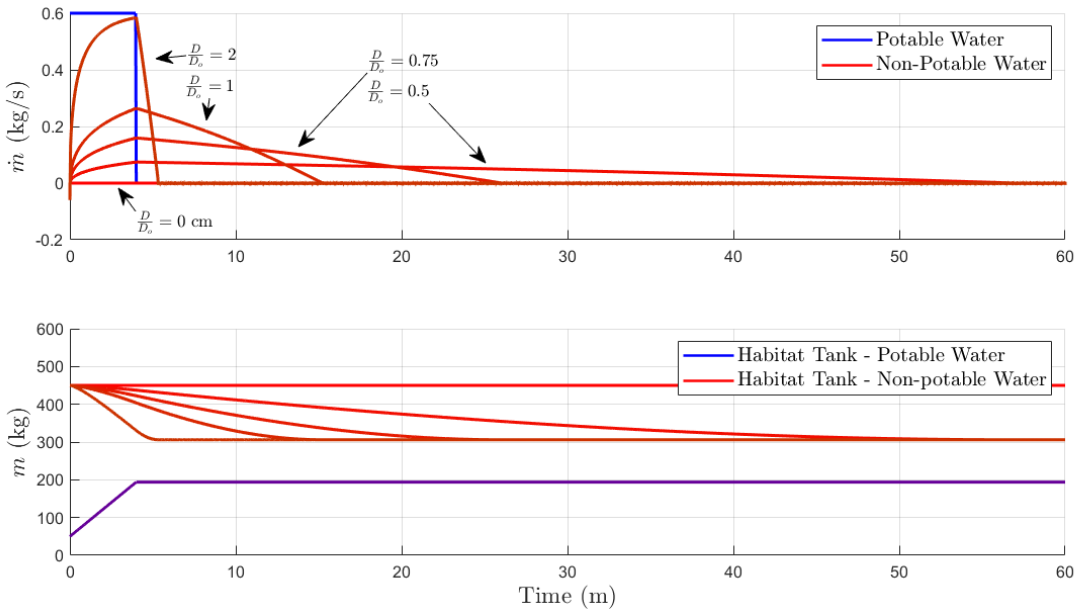

Figure 10: The total tank mass and mass flow rate over time of the uncontrolled system.

will improve the fidelity of this scenario in order to explore these dynamics.

Figure 10 illustrates the relationship between the pumped, potable water in blue and the various diameters of non-potable water in different shades of red. The radial offset in Figure 10 corresponding to larger diameters reveals a low peak offset of only around 1%, while the maximum offset is on the order of 3%. These values are, of course, highly dependent on the mass of the transferred liquid as a function of total system mass and mass flow rate, as illustrated by Figure 8.

CONCLUSION

In this paper, the dynamic system of two opposing, pressurized masses containing fluids that share a common boundary is modeled, studied, and ultimately stabilized using a passive configuration. The performance of this stabilization as a function of total system mass and return line pipe diameter is explored, and it is shown that total system mass has a nonlinear relationship with the offset of the center of mass relative to the geometric center of the configuration. Return pipe diameter relative to pumped fluid diameter strongly affects the stabilization time of the system, with return pipe diameters exceeding pump pipe diameter inducing some slosh effects, though these are likely quickly damped out in real-world scenarios.

Future work will remove many of the assumptions made in this paper to better understand the behavior of a more realistic system, including laminar flow, constraints on axial motion only, constant acceleration and angular velocity, and the assumption of isolated, incompressible fluids in a perfectly closed tank. It will also test the robustness of passive stabilization methods in the presence of external perturbations and usage of a guidance and control algorithm. Furthermore, the extensibility of this approach to slosh dynamics will likewise be explored in order to better understand control methodology with application to on-orbit refueling and large vehicles in microgravity environments.

REFERENCES

[1] D. V. Byrnes, J. M. Longuski, and B. Aldrin, "Cycler orbit between earth and mars," *Journal of Spacecraft and Rockets*, vol. 30, pp. 334–336, 1993.

[2] R. S. Taylor, "A passive pendulum wobble damping system for a manned rotating space station," *AIAA Journal of Spacecraft and Rockets*, vol. 3, p. 8, 1966.

[3] W. Wei, P. Marston, D. Thiessen, C. Niederhaus, D. Truong, and M. Marr-Lyon, "Passive and active stabilization of liquid bridges in low gravity," in *2001 Conference and Exhibit on International Space Station Utilization*, 2012.

[4] Z. Guang, B. Xingzi, and L. Bin, "Optimal deployment of spin-stabilized tethered formations with continuous thrusters," *Nonlinear Dynamics*, vol. 95, pp. 2143–2162, 2018.

[5] K. M. Martin, D. F. Landau, and J. M. Longuski, "Method to maintain artificial gravity during transfer maneuvers for tethered spacecraft," *Acta Astronautica*, vol. 120, pp. 138–153, 2016.

[6] L. D. Peterson, E. F. Crawley, and R. J. Hansman, "Nonlinear fluid slosh coupled to the dynamics of a spacecraft," *AIAA Journal*, vol. 27, no. 9, pp. 1230–1240, 1989.

[7] K. M. Martin, D. F. Landau, and J. M. Longuski, "Method to maintain artificial gravity during transfer maneuvers for tethered spacecraft," *Acta Astronautica*, vol. 120, pp. 138–153, 2016.

[8] A. jun Li, H. chang Tian, and C. qing Wang, "Fixed-time terminal sliding mode control of spinning tether system for artificial gravity environment in high eccentricity orbit," *Acta Astronautica*, vol. 177, pp. 834–841, 2020.

[9] A. Bukley, W. Paloski, and G. Clément, *Physics of Artificial Gravity*, pp. 33–58. New York, NY: Springer New York, 2007.

[10] G. K. O'Neill, *The High Frontier: Human Colonies in Space*. Collector's Guide Publishing, Inc., 1976.

[11] A. Guzman, "Building a better future in orbit," Jun 2022.

[12] H. Wen, D. Jin, and H. Hu, "Advances in dynamics and control of tethered satellite systems," *Acta Mechanica Sinica*, vol. 24, pp. 229–241, 2008.

[13] R. Hoyt, B. Gilchrist, and S. Bilén, "Systems considerations for space tether missions," in *AIAA SPACE 2009 Conference & Exposition*, 09 2009.

[14] R. C. Hibbeler, *Fluid Mechanics*. Pearson, 2014.

[15] N. Nobari and A. Misra, "Satellite attitude stabilization using four fluid rings in a pyramidal configuration," in *AIAA/AAS Astrodynamics Specialist Conference*, 2012.